

Lab on a Chip

Accepted Manuscript



This is an *Accepted Manuscript*, which has been through the Royal Society of Chemistry peer review process and has been accepted for publication.

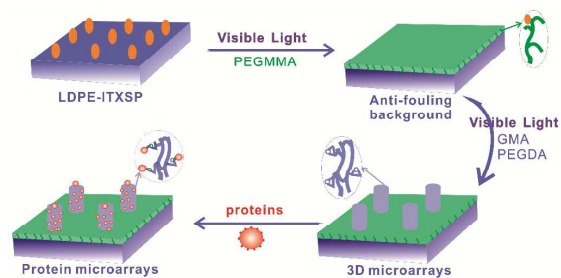
Accepted Manuscripts are published online shortly after acceptance, before technical editing, formatting and proof reading. Using this free service, authors can make their results available to the community, in citable form, before we publish the edited article. We will replace this *Accepted Manuscript* with the edited and formatted *Advance Article* as soon as it is available.

You can find more information about *Accepted Manuscripts* in the [Information for Authors](#).

Please note that technical editing may introduce minor changes to the text and/or graphics, which may alter content. The journal's standard [Terms & Conditions](#) and the [Ethical guidelines](#) still apply. In no event shall the Royal Society of Chemistry be held responsible for any errors or omissions in this *Accepted Manuscript* or any consequences arising from the use of any information it contains.

Table of contents entry.

Colour graphic:



Text:

Create 3D protein microarrays with an anti-fouling background and a high protein capacity by photo-induced surface sequential controlled/living graft polymerization.

Cite this: DOI: 10.1039/c0xx00000x

www.rsc.org/xxxxxx

ARTICLE TYPE

An Extremely Simple Method for Fabricating 3D Protein Microarrays with an Anti-Fouling Background and High Protein Capacity

Zhifeng Lin^a, Yuhong Ma^b, Changwen Zhao^{*a}, Ruichao Chen^a, Xing Zhu^a, Lihua Zhang^a, Xu Yan^a, Wantai Yang^{*a,b}

^aState Key Laboratory of Chemical Resource Engineering, Beijing University of Chemical Technology, Beijing, 100029, China

^bKey Laboratory of Carbon Fiber and Functional Polymers, Ministry of Education, College of Materials Science and Engineering, Beijing University of Chemical Technology, Beijing 100029, China

ABSTRACT. Protein microarrays have become vital tools for various applications in biomedicine and bio-analysis during the past decade. The intense requirements for a lower detection limit and industrialization in this area have resulted in a persistent pursuit to fabricate protein microarrays with a low background and high signal intensity via simple methods. Here, we report on an extremely simple strategy to create three-dimensional (3D) protein microarrays with an anti-fouling background and a high protein capacity by a photo-induced surface sequential controlled/living graft polymerization developed in our lab. According to this strategy, “dormant” groups of isopropyl thioxanthone semipinacol (ITXSP) were first introduced on a polymeric substrate through ultraviolet (UV)-induced surface abstraction of hydrogen, followed by a coupling reaction. Under visible light irradiation, the ITXSP groups were photolyzed to initiate a surface living graft polymerization of poly(ethylene glycol) methyl methacrylate (PEGMMA), thus introducing PEG brushes on the substrate to generate a full anti-fouling background. Due to the living nature of this graft polymerization, there were still ITXSP groups on the chain ends of the PEG brushes. Therefore, by an *in situ* secondary living graft cross-linking copolymerization of glycidyl methacrylate (GMA) and polyethylene glycol diacrylate (PEGDA), we could finally plant height-controllable cylinder microarrays of a 3D PEG network containing reactive epoxy groups onto the PEG brushes. Through a commonly used reaction of amine and epoxy groups, the proteins could readily be covalently immobilized onto the microarrays. This delicate design aims to overcome two universal limitations in protein microarrays: a full anti-fouling background can effectively eliminate noise caused by non-specific absorption and a 3D reactive network provides a larger protein-loading capacity to improve signal intensity. The results of non-specific protein absorption tests demonstrated that the introduction of PEG brushes greatly improved the anti-fouling property of the pristine low-density polyethylene (LDPE), for which the absorption to bovine serum albumin was reduced by 83.3%. Moreover, the 3D protein microarrays exhibited a higher protein capacity than the controls to which were attached the same protein on PGMA brushes and monolayer epoxy functional groups. The 3D protein microarrays were used to test the immunoglobulin G (IgG) concentration in human serum, suggesting that they could be used for biomedical diagnosis, which indicates that more potential bio-applications could be developed for these protein microarrays in the future.

INTRODUCTION

Protein microarrays, also known as protein chips, are micro-fabricated functional surfaces that can bind to different proteins in a high-density format¹. Through protein-protein, protein-nucleic acid, protein-lipid and protein-small molecules^{2, 3} interactions, protein microarrays provide an efficient way to detect the direct information on bio-macromolecules in high throughput^{4, 5}.

For the fabrication of satisfactory protein microarrays, a low fluorescence background is a critical issue^{6, 7}. Currently, the commonly used solid support materials of protein microarrays contain glass, metals and polymers. Polymer support materials are potentially valuable alternatives to inorganic surfaces for their inexpensive and easy processing properties⁸⁻¹⁰. However, major disadvantages of polymers are their low surface energy and chemical inertness¹¹⁻¹³. The low surface energy of hydrophobic polymers causes them to severely suffer from bio-fouling of proteins, bacteria and other biomolecules^{12, 13}. As a result,

polymer protein microarrays exhibit a high background fluorescence, and immobilized proteins can be inactivated because of denaturalization and steric occlusion^{8, 14, 15}.

The tethering of PEG brushes or PEG hydrogel is an efficient way to improve surface anti-fouling properties¹⁵. These PEG-based surfaces offer a wealth of advantages, such as being highly hydrophilic, nontoxic, nonimmunogenic, and more significantly, with an ability to resist non-specific protein adsorption¹⁶⁻¹⁸. However, a new problem has emerged with such PEG-ylated surfaces: a difficulty to further fabricate protein microarrays on this resisting protein absorption surface.

Another critical issue when preparing satisfactory protein microarrays is to elevate the protein-binding capacity in the array area, which mainly depends on surface modification strategies. Presently, monolayers of reactive groups, polymer brushes and 3D polymer network are the three common modification methods used to fabricate substrates with protein microarrays¹⁹⁻²². Comparatively, the preparation of protein microarrays with 3D structures provides the most essential advantages^{23, 24}. The 3D

protein microarrays exhibit a higher protein-binding capacity and simultaneously provide a longer spacing between immobilized molecules²⁵⁻²⁷. Besides, a 3D network gel contains a large amount of water²⁸, which gives rise to a soft landing and aqueous surrounding for the protein, and prevents the irreversible protein denaturalization^{29,30}.

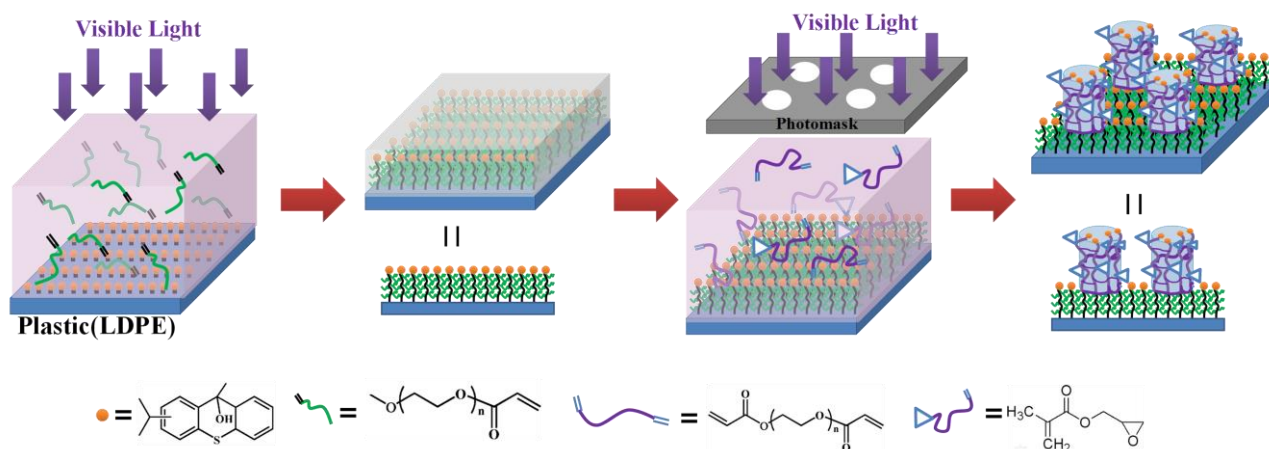
Based on the above analysis and considering the practical application, surface-initiated controlled/living graft polymerization may be the most suitable method to fabricate 3D network protein microarrays on polymer surfaces with an anti-fouling background of PEG brushes. This technique allows further graft polymerization on the first grafting layer, which could be utilized to introduce reactive microarrays on the anti-fouling background for protein binding. Among available surface-initiated controlled/living graft polymerization techniques, the ones most commonly are ATRP, RAFT and NMP^{19,31,32}. However, these methods require a complicated series of pretreatment reactions to introduce functional groups for initiator immobilization such as the modification of the chemically inert polymer surface involved. Moreover, patterning microarrays on a fully modified background also incurs additional masking steps. Therefore, further efforts are needed to explore novel simple controlled/living graft polymerization methods that could easily fabricate patterns on a first graft layer^{31,32}.

In 1996, Yang and Rånby³³ reported on a surface radical living graft approach to introduce polymer brushes and this work was further developed by Ma and coworkers³⁴. Unlike the other living graft polymerization technologies, the photo-induced method can directly transfer the inert C-H bonds to the liable C-C bonds or grafting chains with reversible dormant groups. With this

technique, the graft area and graft polymer chain length can be readily controlled³¹. Recently, this method was further expanded to a visible light-induced surface living graft polymerization system³⁵. In that work, isopropyl thioxanthone (ITX) was photoreduced under UV light and sequentially coupled to the surface of polymeric substrates to produce an isopropyl thioxanthone semipinacol (ITXSP) dormant group. The immobilized ITXSP group could then serve as a reactive site to initiate surface grafting of vinyl monomers such as glycidyl methacrylate (GMA) under visible light.

In the present work, we further demonstrate that this visible light-induced polymerization method can be applied in order to directly fabricate high-performance protein microarrays with high protein capacity (moles of protein per unit area) and low non-specific adsorption on the background. The chemical strategy and procedure is shown in Scheme 1. With low density polyethylene (LDPE) film as the model of polymeric substrates, ITXSP was firstly coupled to the surface³⁶. Subsequently, PEG brushes were grafted to the surface by visible light-induced grafting polymerization to achieve an anti-fouling background. Finally, functional cylinder arrays carrying epoxy groups were created on the anti-fouling surface by living grafting cross-linking copolymerization.

Proteins could be easily immobilized in the 3D cylinder arrays via reaction of their amine groups with epoxy groups. Results indicated that the antifouling background surface significantly reduced the background fluorescence intensity, and the 3D protein microarrays exhibited a higher signal fluorescence intensity as opposed to protein microarrays prepared from polymer brushes and monolayer functional groups.



Scheme 1. Schematic illustration of the surface modification strategies (1, PEG brushes were grafted onto the surface to achieve an anti-fouling background; 2, functional cylinder arrays carrying epoxy groups were created on the anti-fouling surface to immobilize proteins).

EXPERIMENTAL SECTION

Materials

Low density polyethylene (LDPE) with a thickness of about 60 μm was obtained from Beijing Plastic Factory. All LDPE films were cut into square shapes with a length of 3 cm. They were subsequently extracted with acetone for 12 h and then dried in a

vacuum oven at 25 $^{\circ}\text{C}$ until a constant weight. Isopropyl thioxanthone (ITX, >99%) was purchased from Th-unis Insight corporation. Poly (ethylene glycol) diacrylate (PEGDA) with an average M_n of 575 and poly(ethylene glycol) methyl methacrylate (PEGMMA) with an average M_n of 950 were purchased from Sigma-Aldrich Chemical Corporation. Glycidyl methacrylate (GMA) was obtained from Beijing Yanshan Petrochemical Company and used after distillation under vacuum. Bovine

Serum Albumin (BSA), FITC-BSA, RBITC-conjugated goat *anti*-rabbit IgG (RBITC-IgG), FITC-conjugated rabbit *anti*-goat IgG (FITC-*anti*-IgG), goat *anti*-human IgG (*anti*-human IgG), human IgG, and RBITC-conjugated goat *anti*-human IgG (RBITC-*anti*-human IgG) were purchased from Bossbio Corporation and used without further purification. An epoxy-modified slide was purchased from GencBio Corporation.

Introducing PEG Brushes

Firstly, 150 μL of 30 wt% ITX solution in acetone was added to and spread evenly over the surface of the LDPE film. A thin flat solution layer was formed by placing a quartz plate (weight 45 g) on the top to exert a certain pressure. This setup then underwent 3 minutes of UV light irradiation (high-pressure mercury lamp, 9 mW/cm^2 at a wavelength of 254 nm) at room temperature. Subsequently, the films were washed with a large amount of acetone and were Soxhlet extracted with acetone for 12 h in the dark. Finally, the films were dried in a vacuum oven at 25 $^\circ\text{C}$ for 2 h. All samples were stored in the dark. These films were denoted LDPE-ITXSP.

To conduct the graft polymerization, PEGMMA was dissolved in ultrapure water to form a 30 wt% PEG monomer solution. Then, 150 μL of this PEG solution was added to the surface of the LDPE-ITXSP films. The PEG solution was spread evenly over the surface where a thin flat solution layer was formed by placing a quartz plate (weight 45 g) on the top. This sandwich setup was placed under the irradiation of visible light (500 W xenon lamp equipped with a filter to allow a bandpass of 380–700 nm, 10 mW/cm^2 at a wavelength of 420 nm) at room temperature for 30 minutes unless noted otherwise. The PEG-modified films were washed with large amounts of acetone and then Soxhlet extracted with acetone for 12 h in the dark. Subsequently, the films were dried in a vacuum oven at 25 $^\circ\text{C}$ for 2 h. All samples were stored in the dark. The LDPE-*g*-(PEG brush) films are referred to as LDPE-*g*1 in the following.

The anti-fouling performance of LDPE-*g*1 and blank LDPE were tested as follows. A pristine LDPE film, an LDPE-*g*1 film and a hydroxylated glass slide with a size of 9 cm^2 were immersed in 5 mL of 1 mg/mL BSA solution for 4 h at 37 $^\circ\text{C}$. Then, the substrates were gently washed five times by PBS, and the rinsing fluid and remaining solution were collected and diluted with PBS to 100 mL. Subsequently, a Coomassie Brilliant Blue G-250 reagent was mixed with the BSA solution at a 1:5 volume ratio and incubated for 5 min at room temperature. The absorbance of the BSA solution was then measured at 595 nm by UV-Vis spectrometry. The weight of the protein adsorbed on the substrates was calculated by comparing the absorbance of the mixture with the standard calibration curve. The non-specific protein adsorption was also investigated by fluorescence microscopy. The pristine LDPE film, the LDPE-*g*1 film and the glass slide were immersed in 1 mL of 100 $\mu\text{g}/\text{mL}$ FITC-BSA solution for 4 h at 37 $^\circ\text{C}$, after which they were observed by fluorescence microscopy.

Introducing 3D Functional Cylinder Arrays on PEG brushes

A monomer solution comprising acetone (40 wt%), PEGDA ($M_n = 575$, 20 wt%) and GMA (40 wt%) was prepared, after which 150 μL of it was dropped on LDPE-*g*1. The liquid was

spread evenly over the surface and a thin flat solution layer was formed by placing a quartz plate (weight 45 g) or a metallic photo-mask (weight 20 g) on top. The setup was irradiated with visible light (500-W xenon lamp equipped with a filter to allow a bandpass of 380–700 nm, 10 mW/cm^2 of visible light intensity at wavelength 420 nm) at room temperature, for 60 minutes unless noted otherwise. Finally, the LDPE-*g*-(PEG brush)-*g*-(functional gel) films, denoted LDPE-*g*1-*g*2 below, were washed with large amounts of acetone and Soxhlet extracted with acetone for 12 h in the dark. The films were dried in a vacuum oven at 25 $^\circ\text{C}$ for 2 h. All samples were stored in the dark.

Conjugating Protein into Microarrays

RBITC-IgG and FITC-*anti*-IgG was diluted by PBS solution (0.01 M, pH = 7.4) at a concentration of 0.5 mg/mL. Then 150 μL of RBITC-IgG solution was dropped on the surface of the protein microarray substrates, and they were incubated for 2 h at 30 $^\circ\text{C}$. The film was washed with large amounts of ultrapure water and PBS solution three times. Subsequently, the RBITC-IgG protein microarrays, denoted LDPE-*g*1-*g*2-*Ag* microarrays, were formed. For hybridization of the LDPE-*g*1-*g*2-*Ag* microarrays with *anti*-IgG, 150 μL of FITC-*anti*-IgG solution was dripped on the LDPE-*g*1-*g*2-*Ag* microarrays, and they were incubated for 2 h at 30 $^\circ\text{C}$. Next, the films were washed thoroughly with PBS solution three times and stored in PBS solution in the dark.

Protein microarrays on the epoxy-modified slide which covered the epoxy group layer were formed by spotting protein solution onto the surface. Each point had a diameter of about 80 μm . The brushes of protein microarrays were prepared by the same strategy as the 3D microarrays, while only GMA monomer (60 wt%) was added in the third step instead of the solution of GMA and PEGDA. The substrates' surface topography was observed by AFM. Fluorescence signals were obtained by fluorescence microscopy, and the fluorescence intensity was calculated by the Image-Pro Plus software.

Human IgG Concentration Detection by Protein Microarrays

Firstly, 150 μL of *anti*-human IgG (0.2 mg/mL) was dripped on 8 pieces of substrates and incubated for 2 h at 37 $^\circ\text{C}$ to prepare *anti*-human IgG protein microarrays. Human-IgG was diluted in a PBS solution (0.01 M, pH = 7.4) to concentrations of 100 $\mu\text{g}/\text{mL}$, 200 $\mu\text{g}/\text{mL}$, 300 $\mu\text{g}/\text{mL}$, 500 $\mu\text{g}/\text{mL}$, 600 $\mu\text{g}/\text{mL}$, 800 $\mu\text{g}/\text{mL}$, 1000 $\mu\text{g}/\text{mL}$. Then, 20 μL of the above solutions were dripped onto 7 groups of *anti*-human IgG protein microarrays and were incubated for 2 h at 30 $^\circ\text{C}$. Meanwhile, human serum of unknown concentration was diluted with a PBS solution (0.01M, pH = 7.4) 40 times, after which 150 μL of this solution was dripped onto the surface of the last substrate and incubated for 2 h at 30 $^\circ\text{C}$. All of these microarrays bound with human IgG were washed thoroughly with PBS solution and incubated with 150 μL of RBITC-*anti*-human-IgG solution (0.2 mg/mL) for 2h at 30 $^\circ\text{C}$. Finally, a thorough washing with PBS solution was performed three times and the substrates were stored in PBS solution in the dark. All the samples were analyzed by fluorescence microscopy to record the fluorescence intensity.

Characterization

The surface chemical analysis of reacted samples was carried out with XPS (ESCALAB 250 Thermo Electron Corporation with Al K α X-ray source (1486.6 eV). The core-level signals were obtained at a photoelectron takeoff angle of 75° (with respect to the sample surface). The film samples (0.5 cm \times 0.5 cm) were mounted onto the XPS stage. All binding energies (BEs) were referenced to the C1s peak (BE = 285 eV). The atomic force microscope used for this experiment was a commercially available multimode system with an atomic head of 100 \times 100 μm^2 scan range and the analysis was performed on a CP II (Digital Instruments, USA) equipped with an V-shaped silicon nitride (Si $_3$ N $_4$) cantilever. The instrument was operated in air in contact mode. The drive voltage was above 1V, and the amplitude was below 300 mV. All measurements were taken at a scanning rate of 0.5-1.0 Hz, with a scanning area of 60 \times 60 μm^2 . An average thickness obtained from several force curves at various locations was taken. The protein spotting on the epoxy-modified slide was done by PersonalArrayer (Capital-Bio, China). Fluorescence microscopy (Olympus IX71 microscope, Japan) was performed to collect fluorescence signals and optical photos. Photos of the protein on the substrates were taken after flattening on a clean glass slide.

RESULTS AND DISCUSSION

Preparation of PEG brushes and their anti-fouling performance

An antifouling background plays a significant role in protein microarrays since the fluorescence background signal would be seriously enhanced by non-specific protein adsorption^{18,37}. The tethering of PEG is one of the most commonly used approaches to impart a protein resistance function to a surface¹⁸. It is generally accepted that an increase in hydrophilicity offers a better protein fouling resistance since proteins are hydrophobic in nature¹².

PEG brushes were introduced onto an LDPE surface according to the procedure illustrated in Scheme 1. The elemental compositions of the surface at different stages were investigated by XPS. Figure 1 shows the C 1s core-level of the LDPE, LDPE-ITXSP and LDPE-g1 films. Through XPS peak fitting, the C 1s core-level spectrum of pristine LDPE could be curve-fitted into four main peak components with binding energies of about 282.4, 285, 286.5 and 289 eV, respectively attributable to the C-Si, C-C/H, C-O and O-C=O species.

The C-Si, C-O and O-C=O species in the LDPE film probably resulted from residual silicon release agent and surface thermal oxidation during the processing⁴⁰. The C 1s spectrum of LDPE-ITXSP could be curve-fitted into the neutral hydrocarbon species at 285 eV and C-O species at 286.5 eV. In the case of the LDPE-g1 surface, the C 1s component centered at about 286.5 eV, attributable to the CO species of the grafted PEGMA polymer, became predominant. The C 1s peak component at the BE of 285 eV was ascribed to the CH species of the grafted PEGMA

backbone structure. The minor peak component at the BE of 289 eV, on the other hand, was assigned to the O=C-O species. All the results indicated that the PEG brushes were successfully grafted on the LDPE.

Compared with a pristine LDPE surface and an LDPE-ITXSP surface with water contact angles of respectively 103° and 102° (Figure 1g, h), the surface onto which was grafted the PEG brushes presented a significantly decreased water contact angle of 37° (Figure 1i). This demonstrates the transformation of the surface wetting ability from hydrophobic to hydrophilic after the introduction of the PEG brushes.

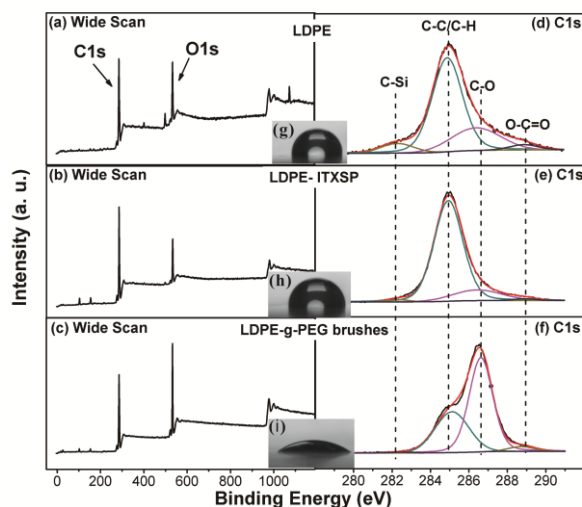


Figure 1. XPS C 1s core-level spectra (d-f) and water contact angles (g-i) of the LDPE, LDPE-ITXSP, LDPE-g1.

Bovine serum albumin (BSA) was used as a model to investigate the non-specific protein adsorption on pristine LDPE, LDPE-g-PEG brushes (LDPE-g1) and a hydroxylated glass slide³⁸. The results were measured by the Bradford assay^{39,40} and fluorescence microscopy¹⁵. A hydroxylated glass slide can be regarded as having perfect non-fouling thanks to its flatness and super hydrophilicity. Figure 2 showed the fluorescence microscopy image of non-specific protein adsorption of FITC-BSA on the investigated substrates. The contact angle (CA) of pristine LDPE was 102.0°, for a fluorescence intensity of 18.3 (a.u.), indicating that it suffered severely from non-specific protein adsorption. In contrast, the C.A was reduced to 37.3° and the fluorescence intensity decreased to 6.5 (a.u.) after the introduction of the PEG brushes, which is to be compared with 2.5 (a.u.) for hydroxylated glass slide and its CA of 11.3°.

Cite this: DOI: 10.1039/c0xx00000x

www.rsc.org/xxxxxx

ARTICLE TYPE

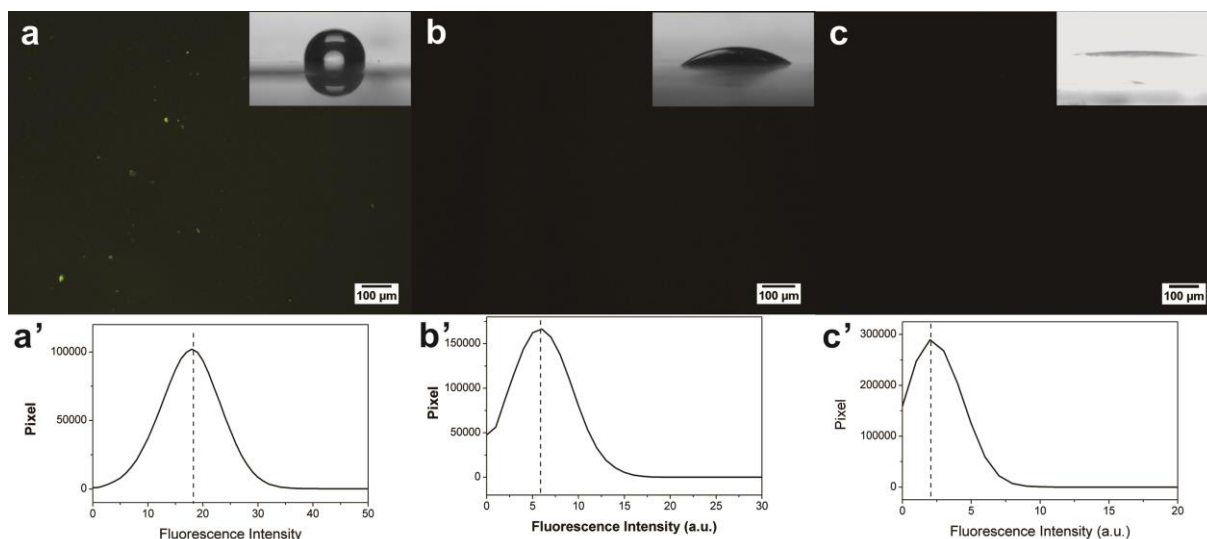


Figure 2. Fluorescence microscopy images of pristine LDPE (a), LDPE-g1 (b) and hydroxylated glass slide (c) after the non-specific FITC-BSA adsorption. (a'-c') Image histogram of the fluorescence intensity by Image-Pro Plus 6.0 (IPP 6.0).

The Bradford assay was used to quantitatively measure the amount of BSA adsorbed on these surfaces and the results can be seen in Figure 3. Among the substrates, the pristine LDPE had the highest non-specific BSA adsorption of 6.42 $\mu\text{g}/\text{cm}^2$. After modification with the PEG brushes, the adsorption of LDPE-g1 was decreased to 1.07 $\mu\text{g}/\text{cm}^2$, which was close to the 1.01 $\mu\text{g}/\text{cm}^2$ of the hydroxylated glass slide. Compared to pristine LDPE, the non-specific absorption of BSA for the LDPE-g1 substrate was reduced by 83.3%. This significant decrease demonstrated that LDPE-g1 could act as a qualified anti-fouling background for further modifications.

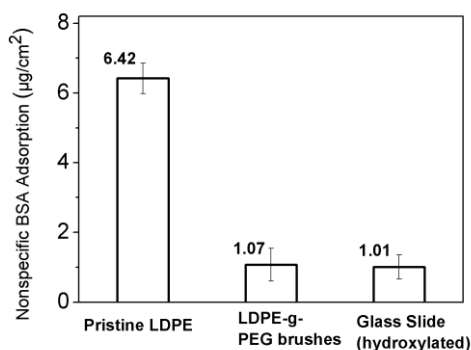


Figure 3. BSA adsorption on the surfaces after treatment with 1.0 mg/mL of pure BSA solutions for 4 h ($n = 4$).

Fabrication of 3D Functional Cylinder Arrays and Binding with Proteins

Since ITXSP was still present on the LDPE-g1 surface, we could readily fabricate a 3D functional network pattern on it.

Under the irradiation of visible light with a photo-mask, the dormant species on the surface were regionally re-activated, and living graft cross-linking copolymerization of GMA and PEGDA could be performed at room temperature. Figure 4 shows the wide scan and C 1s core-level spectra of LDPE-g1-g2 and LDPE-g1-g2-Ag (protein microarrays). The [C/O] ratio of the LDPE-g1-g2 film was 2.61:1, which was higher than that of the LDPE-g1 film since GMA and PEGDA have higher [C/O] ratios than PEGMMA (2:1 for PEGDA was, 2.33:1 for GMA, and 1.82:1 for PEGMMA). The O-C=O species components of LDPE-g1-g2 were 3.93 %, which is higher than the 0.42 % of LDPE-g1. This was due to both GMA and PEGDA having higher contents of O-C=O species, indicating that PEGDA and GMA were introduced onto the surface. The [C/O] ratio of LDPE-g1-g2-Ag was 3.04, and the signal of N (BE = 398.4 eV) also appeared, indicating that the protein was successfully immobilized on the surface.

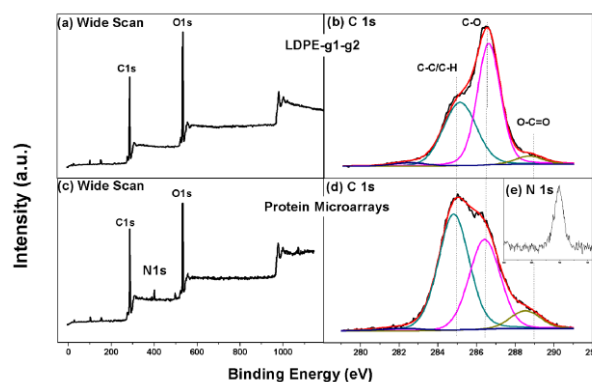


Figure 4. XPS wide scan (a, c) and C 1s core-level spectra (b, d) of LDPE-g1-g2 and LDPE-g1-g2-Ag (c, d). N 1s core-level spectrum (e) of LDPE-g1-g2-Ag.

The surface topography of the cylinder arrays was observed by AFM. As shown in Figure 5, 3D cylindrical patterns with widths of about 45.6 and 22.1 μm were reproduced on the LDPE-g1 surface. These values were wider than the real circles (40 and 20 μm) on the mask. This sidewall distortion was believed to be

caused by a diffraction effect in the photolithography. The thicknesses of the microarrays were determined to be 1.96 μm and 2.13 μm for those with diameters of 45.6 and 22.1 μm respectively, confirming the ability of our strategy to form stand-alone 3D structures on an anti-fouling surface.

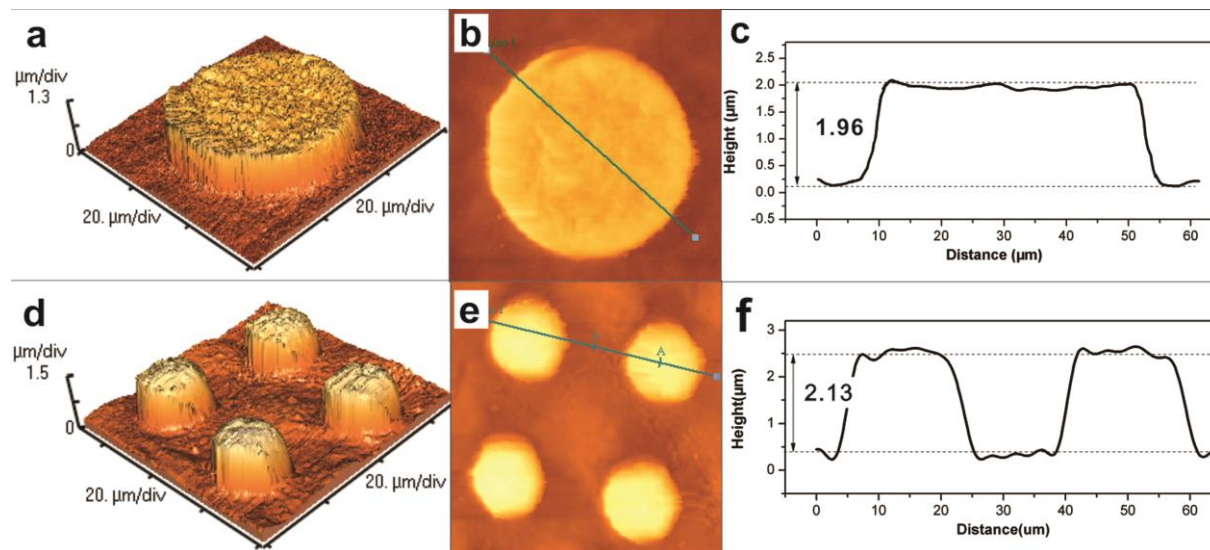


Figure 5. (a, b, d, e) AFM images of the microarray substrates. (c, f) AFM image height analysis of b and e. The monomer solution, composed of acetone (40 wt%), PEGDA ($M_n = 575$, 20 wt%) and GMA(40 wt%), reacted at room temperature for 60 minutes.

To demonstrate the superiority of 3D protein microarrays to those fabricated from polymer brushes and monolayer functional groups, RBITC-labeled IgG was conjugated to these substrates and the fluorescence intensity was measured and is shown in Figure 6. It was observed that the fluorescence intensity of 3D protein microarrays was 120 (a.u.), which was significantly higher than the value of 37 (a.u.) of the brush protein microarrays and the value of 29 (a.u.) of monolayer protein microarrays. This indicated that 3D protein microarrays have a higher protein capacity than the other two protein microarrays. Moreover, the fluorescence spot of the 3D microarrays showed well-defined shapes, which meets the prerequisite for practical applications of protein microarrays. The higher fluorescence intensity of 3D

protein microarrays could be attributed to the fact that its 3D structure allows it to carry more epoxy functional groups per unit area than polymer brushes and monolayer functional groups.

To further determine the function of the PEG brushes, we also prepared PGMA brushes directly on the LDPE-ITXSP to bind RBITC-labeled IgG. Its fluorescent images are shown in Figure 6d. Contrary to the 3D protein microarray with a PEG background, the protein microarray without an anti-fouling background severely suffered from non-specific protein absorption and the fluorescent intensity of these microarrays decreased to 22 (a.u.), which reconfirmed that PEG brushes on an anti-fouling background could effectively reduce non-specific protein adsorption on the substrate.

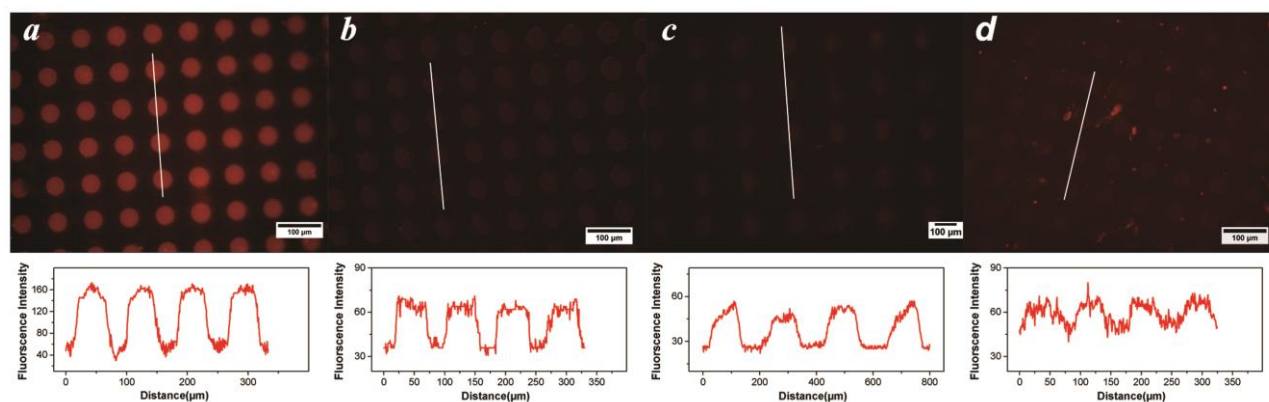


Figure 6. Microscopy images and fluorescence intensity analyses of protein microarrays. (a) 3D protein microarrays, with an average cylinder height of 1.96 μm . (b), brush protein microarrays, with an average cylinder height of 0.89 μm . (c), monolayer protein microarrays, flat surface. (d) 3D protein microarrays without an antifouling PEG background, with an average cylinder height of 0.83 μm . The fluorescence intensity was counted by Line Profile of Image-Pro Plus 6.0 software.

Cite this: DOI: 10.1039/c0xx00000x

www.rsc.org/xxxxxx

ARTICLE TYPE

Effect of PEGDA Content on Immobilization Capacity

In order to immobilize proteins with 3D functional cylinder arrays, a robust and stable 3D network structure and an ease of reaction with proteins are important issues. Here, PEGDA was used as a cross-linking agent, while GMA was employed as a functional monomer to introduce epoxy groups into the cylinders. The ratio of PEGDA to GMA has a significant influence on the binding capacity of 3D microarrays to proteins. A proper amount of PEGDA could ensure that the microarrays cross-linked so as to give rise to a tough 3D structure with appropriate height for carrying more epoxy groups. Moreover, a moderate copolymerization with PEGDA could effectively space epoxy groups to increase their reaction efficiency with large sizes of proteins.

However, an excessive PEGDA content would cause two negative results: a considerable reduction of the amount of epoxy groups and an increased cross-linking density of the 3D microarrays, which may hinder the protein from diffusing into the network and reacting with the epoxy groups. As shown in Figure 7, when no PEGDA was added, it was only possible to obtain PGMA brushes with a thickness of 0.89 μm and, after immobilization of RBITC-labeled IgG, a fluorescence intensity of 37 (a.u.). While the fluorescence intensity and height increased to 69 (a. u.) and 1.98 μm , respectively, after adding 12 wt% of PEGDA, indicating that more labeled IgG were immobilized into the 3D arrays compared to PGMA brushes. Larger amount of PEGDA made the microarrays have a higher height for carrying more epoxy groups. When further increasing the PEGDA content from 12 wt% to 60 wt% (decreasing the GMA content from 48 wt% to 0 wt%), the heights of the 3D cylinder microarrays were almost constant at 1.96 μm . However, the change in fluorescence intensity was quite dramatic, first increasing and then decreasing. The highest value of the fluorescence intensity was around 122 (a. u.) with a PEGDA concentration of 30 wt%. When increasing the PEGDA content from 12 wt% to 20 wt%, PEGDA spaced epoxy groups so as to increase the reaction efficiency of epoxy groups. When increasing the PEGDA content from 20 wt% to 36 wt% (decreasing the GMA content from 40 wt% to 24 wt%), much less amount and higher reaction efficiency of epoxy groups function together, led the fluorescence intensity to be constant at around 120 (a. u.). When the PEGDA concentration increased from 36% to 60%, the amount of epoxy groups carried by microarrays reduced significantly, the fluorescence intensity showed a drastic decrease from 118 (a. u.) to zero. Therefore, the optimized concentration range for the selection of a proper height structure and high immobilized protein capacity was between 20 wt% to 36 wt% of PEGDA.

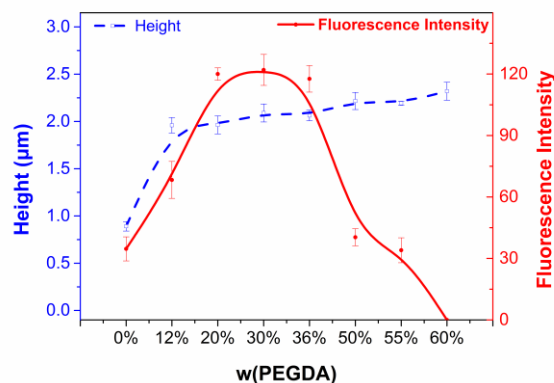


Figure 7. Fluorescence intensity of a protein microarray and height of a 3D microarray for different PEGDA weight percentages (wt%) of 0, 12, 20, 30, 36, 50, 55, 60. W(monomers) = 60wt%, w (solvent) = 40wt%. (n=3).

Controlling Immobilization Capacity by Height Adjustment of the 3D Microarrays

After determining the proper monomer ratios, we further investigated the effect of the height of the cylinders on the immobilization density of the proteins. For LDPE-g1-g2, the protein binding capacity per unit area was mainly determined by the density of the epoxy groups which was associated with the height of the cylinders. For this visible light-induced controlled/living graft polymerization system, the cylinder heights could be easily controlled. As shown in Figure 8, the height of the functional 3D microarrays increased from 0 to 3.2 μm with an increasing irradiation time from 0 to 90 minutes, confirming that the polymerization proceeded in a controlled manner. As the height grew, the amount of epoxy functional groups increased indicating that more proteins could be immobilized on the substrate. It was observed that as the height of the cylinders grew to 3.2 μm , the fluorescence intensity also increased to 139 (a.u.), implying that the protein capacity of the microarrays could be easily controlled by adjusting the height of the microarrays.

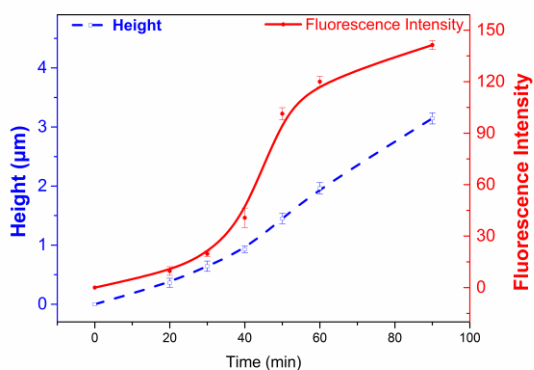


Figure 8. Fluorescence intensity of the protein microarrays and height of the 3D microarrays for different grafting times of 0 min, 20 min, 30 min, 40 min, 50 min, 60 min, 90 min. The monomer solution was composed of acetone (40 wt%), PEGDA (20 wt%) and GMA(40 wt%). (n=3).

Binding 3D IgG microarrays with anti-IgG

RBITC-labeled goat *anti*-rabbit IgG (RBITC-IgG) was used as an antigen model to conjugate with LDPE-*g*1-*g*2 and a specific binding of protein microarrays with the target antibody, FITC-conjugated rabbit *anti*-goat IgG (FITC-*anti*-IgG) was performed. As shown in Figure 9a, well-defined circular red fluorescent signals with diameters of 40 µm appeared after RBITC-IgG was immobilized onto the functional cylinder arrays, indicating that the proteins were successfully immobilized on the surface. After specific interaction with FITC-*anti*-IgG, the microarrays presented well-defined clear green circular fluorescent signals under the excitation of blue light as shown in Figure 9b. These results suggest that the immobilized protein could interact specifically with its target protein.

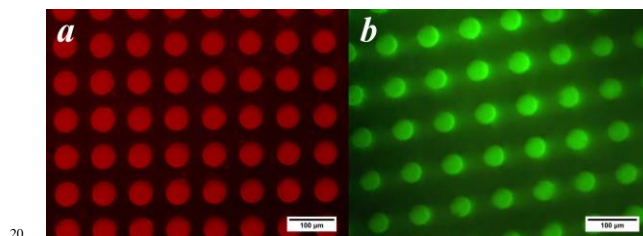
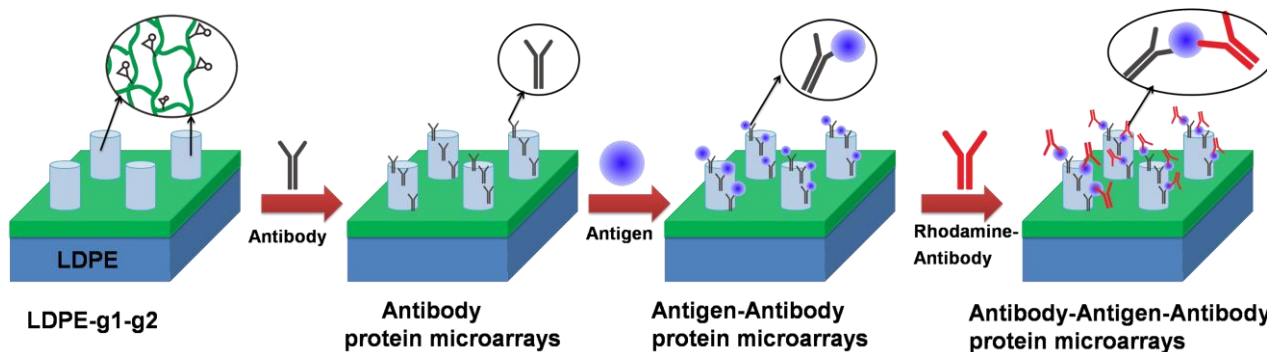


Figure 9. Fluorescent images of RBITC-conjugated goat *anti*-rabbit IgG (a) and FITC-conjugated rabbit *anti*-goat IgG (b).

IgG Assay on 3D Protein Microarrays.

The level of immunoglobulin G (IgG) in serum is one of the key markers for disease diagnosis⁴¹. For example, the serum levels of IgG have been found to be higher in patients with glomerulonephritis than in those without, and patients with alimentary canal cancer and rheumatoid arthritis also demonstrate higher serum levels of IgG⁴².

To verify the function of the 3D protein microarrays upon detection of IgG levels in human serum, we prepared double antibody sandwich microarrays according to Scheme 2. Firstly, *anti*-human IgG was immobilized on the LDPE-*g*1-*g*2 surface and an antibody microarray was formed. Secondly, human IgG was introduced by its specific binding with *anti*-human IgG on the antibody microarray. Thirdly, RBITC-*anti*-human IgG interacted with human IgG on the protein microarray by specific binding to obtain visual results observed by fluorescence microscopy.



Scheme 2. Illustration of double antibody sandwich microarrays to detect IgG levels in human serum.

Based on the knowledge of various human IgG concentrations, a calibration curve of the relationship between the fluorescence intensity with human IgG concentration was firstly plotted by testing various known concentrations of human IgG (Figure 10). After the line-fitting, an equation of fluorescence intensity and IgG concentration for calibration was obtained:

$$FI = 6.67 + 0.115C \quad (1)$$

Where FI was the gray value of the fluorescence signal intensity and C was the IgG concentration. When an unknown

concentration of human serum was tested, the FI was determined to be 38 (a. u.), and the IgG concentration was calculated to be 272.4 µg/mL after dilution 40 times. The real IgG concentration in this human serum sample was 10.9 mg/mL, which was considered a normal level⁴³.

These results indicated that the fluorescence intensity of microarrays was linearly dependent on the concentration of IgG, and the concentration of protein could be tested. All of the above pointed at a great potential for bio-applications on protein microarrays in the future.

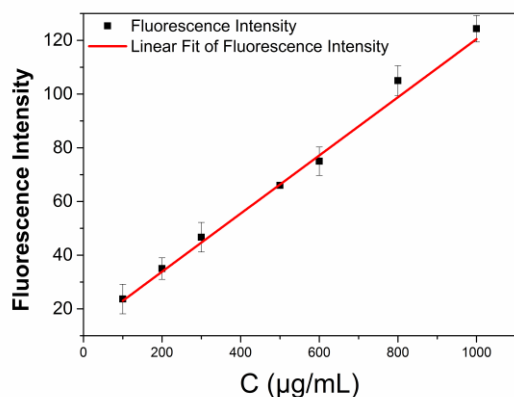


Figure 10. Mean fluorescence signal intensity to different IgG concentrations and its linear fit ($R=0.99$, $n=3$).

CONCLUSION

This article presents a simple method to create 3D protein microarrays with an antifouling background and a high protein capacity via visible light-induced graft polymerization. The successful introduction of a background of PEG brushes and 3D cross-linked cylinders by copolymerization of PEGDA and GMA were confirmed by XPS, water contact angle measurements and AFM characterization. The presence of such a PEG brush background could effectively eliminate non-specific absorption of proteins and thereby offer low background noise. The epoxy groups of the 3D cylinder microdomains could react with amine groups of RBITC-labeled IgG to form protein microarrays, which was verified by fluorescence microscopy. The effect of the PEGDA content on the immobilization density of the proteins was investigated and the optimal PEGDA to GMA ratio was found to be 1 : 1 (w/w). Contrary to protein microarrays fabricated from monolayer functional groups and polymer brushes, 3D protein microarrays have a higher protein capacity. Due to the controlled polymerization of this system, it is facile to control the height of the 3D cylinders and then adjust the immobilization density of the protein. We also demonstrated that IgG levels of human serum could be tested by 3D protein microarrays, suggesting that the technique has great potential for applications in biomedical diagnosis.

Notes and references

Supporting Information

Detailed results and discussion of UV-visible spectra and FTIR characterization; Detailed results and a discussion of growth kinetics research of polymers or copolymers from plastic films and protein incubation time.

Corresponding Author

Wantai Yang^{a,b}, E-mail: yangwt@mail.buct.edu.cn;

Changwen Zhao^a, E-mail: zhaocw@mail.buct.edu.cn;

^aState Key Laboratory of Chemical Resource Engineering, Beijing University of Chemical Technology, Beijing, 100029, China.

^bKey Laboratory of Carbon Fiber and Functional Polymers, Ministry of Education, College of Materials Science and Engineering, Beijing University of Chemical Technology, Beijing 100029, China.

Notes

The authors declare no competing financial interest.

Acknowledgement

The authors are grateful for the financial support from the National Natural Science Foundation of China (Grant No. 51033001, 51221002, 51103009), the National High Technology Research and Development Program (863 Program 2009 AA03Z325) and the Fundamental Research Funds for the Central Universities (ZY1311, ZD1301).

References

- Tao, S. C.; Chen, C. S.; Zhu, H., Applications of protein microarray technology. *Combinatorial Chemistry & High Throughput Screening* 2007, **10**, (8), 706-718.
- Berrade, L.; Garcia, A. E.; Camarero, J. A., Protein Microarrays: Novel Developments and Applications. *Pharmaceutical Research* 2011, **28**, (7), 1480-1499.
- Ramachandran, N.; Hainsworth, E.; Bhullar, B.; Eisenstein, S.; Rosen, B.; Lau, A. Y.; Walter, J. C.; LaBaer, J., Self-assembling protein microarrays. *Science* 2004, **305**, (5680), 86-90.
- Kaushansky, A.; Allen, J. E.; Gordus, A.; Stiffler, M. A.; Karp, E. S.; Chang, B. H.; MacBeath, G., Quantifying protein-protein interactions in high throughput using protein domain microarrays. *Nature Protocols* 2010, **5**, (4), 773-790.
- Zhu, H.; Qian, J., Applications of Functional Protein Microarrays in Basic and Clinical Research. *Advances in Genetics*, Vol 79 2012, **79**, 123-155.
- Kim, D.-N.; Lee, W.; Koh, W.-G., Preparation of protein microarrays on non-fouling and hydrated poly(ethylene glycol) hydrogel substrates using photochemical surface modification. *Journal of Chemical Technology and Biotechnology* 2009, **84**, (2), 279-284.
- Derwinska, K.; Gheber, L. A.; Preininger, C., A comparative analysis of polyurethane hydrogel for immobilization of IgG on chips. *Analytica Chimica Acta* 2007, **592**, (2), 132-138.
- Jonkheijm, P.; Weinrich, D.; Schroeder, H.; Niemeyer, C. M.; Waldmann, H., Chemical Strategies for Generating Protein Biochips. *Angewandte Chemie-International Edition* 2008, **47**, (50), 9618-9647.
- Pu, Q.; Oyesanya, O.; Thompson, B.; Liu, S.; Alvarez, J. C., On-chip micropatterning of plastic (cyclic olefin copolymer, COC) microfluidic channels for the fabrication of biomolecule microarrays using photografting methods. *Langmuir* 2007, **23**, (3), 1577-1583.
- Li, Y.; Wang, Z.; Ou, L. M. L.; Yu, H.-Z., DNA detection on plastic: Surface activation protocol to convert polycarbonate substrates to biochip platforms. *Analytical Chemistry* 2007, **79**, (2), 426-433.
- Chen, H.; Yuan, L.; Song, W.; Wu, Z.; Li, D., Biocompatible polymer materials: Role of protein-surface interactions. *Progress in Polymer Science* 2008, **33**, (11), 1059-1087.
- Rana, D.; Matsuura, T., Surface Modifications for Antifouling Membranes. *Chemical Reviews* 2010, **110**, (4), 2448-2471.
- Xu, L.-C.; Siedlecki, C. A., Effects of surface wettability and contact time on protein adhesion to biomaterial surfaces. *Biomaterials* 2007, **28**, (22), 3273-3283.
- Wilson, D. S.; Nock, S., Functional protein microarrays. *Current Opinion in Chemical Biology* 2002, **6**, (1), 81-85.
- Li, M.; Neoh, K. G.; Xu, L. Q.; Wang, R.; Kang, E.-T.; Lau, T.; Olszyna, D. P.; Chiong, E., Surface Modification of Silicone for Biomedical Applications Requiring Long-Term Antibacterial, Antifouling, and Hemocompatible Properties. *Langmuir* 2012, **28**, (47), 16408-16422.
- Cretich, M.; Pirri, G.; Damin, F.; Solinas, I.; Chiari, M., A new polymeric coating for protein microarrays. *Analytical Biochemistry* 2004, **332**, (1), 67-74.
- Gupta, N.; Lin, B. F.; Campos, L.; Dimitriou, M. D.; Hikita, S. T.; Treat, N. D.; Tirrell, M. V.; Clegg, D. O.; Kramer, E. J.; Hawker, C. J., A versatile approach to high-throughput microarrays using thiol-ene chemistry. *Nature Chemistry* 2010, **2**, (2), 138-145.
- Banerjee, I.; Pangule, R. C.; Kane, R. S., Antifouling Coatings: Recent Developments in the Design of Surfaces That Prevent Fouling by Proteins, Bacteria, and Marine Organisms. *Advanced Materials* 2011, **23**, (6), 690-718.

- 19 Barbey, R.; Kauffmann, E.; Ehrat, M.; Klok, H.-A., Protein Microarrays Based on Polymer Brushes Prepared via Surface-Initiated Atom Transfer Radical Polymerization. *Biomacromolecules* 2010, **11**, (12), 3467-3479.
- 20 Angenendt, P., Progress in protein and antibody microarray technology. *Drug Discovery Today* 2005, **10**, (7), 503-511.
- 21 Scheicher, S. R.; Kainz, B.; Koestler, S.; Reitingner, N.; Steiner, N.; Dittbacher, H.; Leitner, A.; Pum, D.; Sleytr, U. B.; Ribitsch, V., 2D crystalline protein layers as immobilization matrices for the development of DNA microarrays. *Biosensors & Bioelectronics* 2013, **40**, (1), 32-37.
- 22 Li, C. Y.; Xu, F. J.; Yang, W. T., Simple Strategy to Functionalize Polymeric Substrates via Surface-Initiated ATRP for Biomedical Applications. *Langmuir* 2013, **29**, (5), 1541-1550.
- 23 Macanovic, A.; Marquette, C.; Polychronakos, C.; Lawrence, M. F., Impedance-based detection of DNA sequences using a silicon transducer with PNA as the probe layer. *Nucleic Acids Research* 2004, **32**, (2).
- 24 Wu, P.; Hogrebe, P.; Grainger, D. W., DNA and protein microarray printing on silicon nitride waveguide surfaces. *Biosensors & Bioelectronics* 2006, **21**, (7), 1252-1263.
- 25 Zubitsova, Z. I.; Zubitsov, D. A.; Sawateeva, E. N.; Stomakhin, A. A.; Chechetkin, V. R.; Zasedatelev, A. S.; Rubina, A. Y., Hydrogel-based protein and oligonucleotide microchips on metal-coated surfaces: Enhancement of fluorescence and optimization of immunoassay. *Journal of Biotechnology* 2009, **144**, (2), 151-159.
- 26 Zubitsov, D. A.; Savvateeva, E. N.; Rubina, A. Y.; Pan'kov, S. V.; Konovalova, E. V.; Moiseeva, O. V.; Chechetkin, V. R.; Zasedatelev, A. S., Comparison of surface and hydrogel-based protein microchips. *Analytical Biochemistry* 2007, **368**, (2), 205-213.
- 27 Zubitsov, D. A.; Ivanov, S. M.; Rubina, A. Y.; Dementieva, E. I.; Chechetkin, V. R.; Zasedatelev, A. S., Effect of mixing on reaction-diffusion kinetics for protein hydrogel-based microchips. *Journal of Biotechnology* 2006, **122**, (1), 16-27.
- 28 Rubina, A. Y.; Dementieva, E. I.; Stomakhin, A. A.; Darii, E. L.; Pan'kov, S. V.; Barsky, V. E.; Ivanov, S. M.; Konovalova, E. V.; Mirzabekov, A. D., Hydrogel-based protein microchips: Manufacturing, properties, and applications. *Biotechniques* 2003, **34**, (5), 1008-1016.
- 29 Ouyang, Z.; Takats, Z.; Blake, T. A.; Gologan, B.; Guymon, A. J.; Wiseman, J. M.; Oliver, J. C.; Davisson, V. J.; Cooks, R. G., Preparing protein microarrays by soft-landing of mass-selected ions. *Science* 2003, **301**, (5638), 1351-1354.
- 30 Rubina, A. Y.; Pan'kov, S. V.; Dementieva, E. I.; Pen'kov, D. N.; Butygin, A. V.; Vasiliskov, V. A.; Chudinov, A. V.; Mikheikin, A. L.; Mikhailovich, V. M.; Mirzabekov, A. D., Hydrogel drop microchips with immobilized DNA: properties and methods for large-scale production. *Analytical Biochemistry* 2004, **325**, (1), 92-106.
- 31 Ma, Y.; Liu, L.; Yang, W., Photo-induced living/controlled surface radical grafting polymerization and its application in fabricating 3-D micro-architectures on the surface of flat/particulate organic substrates. *Polymer* 2011, **52**, (19), 4159-4173.
- 32 Barbey, R.; Lavanant, L.; Paripovic, D.; Schuewer, N.; Sugnaux, C.; Tugulu, S.; Klok, H.-A., Polymer Brushes via Surface-Initiated Controlled Radical Polymerization: Synthesis, Characterization, Properties, and Applications. *Chemical Reviews* 2009, **109**, (11), 5437-5527.
- 33 Wantai, Y.; Rånby, B., Radical Living Graft Polymerization on the Surface of Polymeric Materials. In a, a ed.; a, Ed. a: *Macromolecules*, 1996; Vol. **29**, 3308-3310, p a.
- 34 Ma, H.; Davis, R. H.; Bowman, C. N. A novel sequential photoinduced living graft polymerization. *Macromolecules* 2000, **33** (2), 331-335
- 35 Bai, H.; Huang, Z.; Yang, W., Visible Light-induced Living Surface Grafting Polymerization for the Potential Biological Applications. *Journal of Polymer Science Part a-Polymer Chemistry* 2009, **47**, (24), 6852-6862.
- 36 Li, C.; Glidle, A.; Yuan, X.; Hu, Z.; Pülleine, E.; Cooper, J.; Yang, W.; Yin, H., Creating "Living" Polymer Surfaces to Pattern Biomolecules and Cells on Common Plastics. *Biomacromolecules* 2013, **14**, (5), 1278-1286.
- 37 Gao, C.; Li, G.; Xue, H.; Yang, W.; Zhang, F.; Jiang, S., Functionalizable and ultra-low fouling zwitterionic surfaces via adhesive mussel mimetic linkages. *Biomaterials* 2010, **31**, (7), 1486-1492.
- 38 Cao, X.; Zhang, T.; Deng, J.; Jiang, L.; Yang, W., An Extremely Simple and Effective Strategy to Tailor the Surface Performance of Inorganic Substrates by Two New Photochemical Reactions. *ACS Applied Materials & Interfaces* 2013, **5**, (3), 494-499.
- 39 Bradford, M. M., A rapid and sensitive method for the quantitation of microgram quantities of protein utilizing the principle of protein-dye binding. *Analytical biochemistry* 1976, **72**, 248-54.
- 40 Wang, P.; Tan, K. L.; Kang, E. T.; Neoh, K. G., Surface functionalization of low density polyethylene films with grafted poly(ethylene glycol) derivatives. *Journal of Materials Chemistry* 2001, **12**, (11), 2951-2957
- 41 Imafuku, Y.; Yoshida, H.; Yamada, Y., Reactivity of agalactosyl IgG with rheumatoid factor. *Clinica Chimica Acta* 2003, **334**, (1-2), 217-223.
- 42 Kamei, K.; Nakagawa, A.; Otsuka, Y.; Nakayama, M.; Kobayashi, S.; Matsuoka, K.; Iijima, K., Chronic glomerulonephritis associated with IgG subclass deficiency. *Pediatric Nephrology* 2007, **22** (8), 1229-1234.
- 43 Vendrell, M.; de Gracia, J.; Rodrigo, M. J.; Cruz, M. J.; Alvarez, A.; Garcia, M.; Miravittles, M., Antibody production deficiency with normal IgG levels in bronchiectasis of unknown etiology. *Chest* 2005, **127** (1), 197-204.